Simulation of Length-Preserving Motions of Flexible One Dimensional Objects using Optimization

S. Banerjee[†],
Mechanical Engineering,
Indian Institute of Science,
Bangalore, 560012, India

M. S. Menon[*],
Mechanical Engineering,
Indian Institute of Science,
Bangalore, 560012, India

G. K. Anathasuresh[§],
Mechanical Engineering,
Indian Institute of Science,
Bangalore, 560012, India

A.Ghosal[‡],
Mechanical Engineering,
Indian Institute of Science,
Bangalore, 560012, India

Abstract— *During the motion of one dimensional flexible objects such as ropes, chains, etc., the assumption of constant length is realistic. Moreover, their motion appears to be naturally minimizing some abstract distance measure, wherein the disturbance at one end gradually dies down along the curve defining the object. This paper presents purely kinematic strategies for deriving length-preserving transformations of flexible objects that minimize appropriate 'motion'. The strategies involve sequential and overall optimization of the motion derived using variational calculus. Numerical simulations are performed for the motion of a planar curve and results show stable converging behavior for single-step infinitesimal and finite perturbations[1] as well as multi-step perturbations. Additionally, our generalized approach provides different intuitive motions for various problem-specific measures of motion, one of which is shown to converge to the conventional tractrix-based solution. Simulation results for arbitrary shapes and excitations are also included.*

Keywords: flexible object simulation, hyper-redundant robotics, length preserving transformation, optimization, tractrix.

I. Introduction

Simulation of motion of one dimensional flexible object such as ropes, chains, hair etc., is an active area of research. This problem has its parallel in hyper-redundant robots where the inverse kinematics problem doesn't have unique solution [1-7]. In hyper-redundant robots, for a given motion of the end-effecter, there exist infinitely many solutions for the joint variables and hence additional constraints are imposed to obtain unique inverse kinematics solution. This is known as *resolution of redundancy*. There exist many possible motions for the trailing part of a hyper-redundant chain, whose leading end has a prescribed motion. Choosing a useful solution among them constitutes the problem of *resolution of redundancy*. Such a problem is encountered in the simulation and visualization of motion of flexible objects

such as rope or human hair wherein, given a predefined motion of the *leader* end, how should the *trailing parts* follow. Useful and easily implementable strategies are required to select the motion of the trailing parts from the myriads of redundant possibilities. This has received much attention in the late few decades and there exists a large amount of literature on this topic [8]. Allied topics of tissue simulation for surgical training where flexible objects such as the suturing threads modeled as spring-mass-damper systems [9, 10] are also investigated. In those works equations of motion are solved to predict the motion of parts of the rope. A major difficulty in this approach is the choice of parameters because there is no systematic way of choosing the spring and damping parameters. In another approach [11], Cosserat theory of elastic rods is applied to solve the problem. In another attempt to solve this problem [12], 'key-framing techniques' are used without considering the kinematics or dynamics governing the motion. This method suffers from lack of uniqueness and reality in the simulation so produced. In a recent work, the authors have proposed a purely kinematics/geometric approach based on the classical curve called *tractrix* [13]. The *tractrix* curve was discovered by Leibniz, who obtained the differential equation and analytical solution of the curve. According to Steinhaus H. [14], tractrix is "the *path traced by an object starting off with a vertical offset when it is dragged along by a string of constant length being pulled along a straight horizontal line*". One main property of a tractrix, which makes it a prospective and promising candidate for motion simulation of a moving flexible object, is that for a given motion of the leader, the motions of the trailing parts die down. That is the perturbations tend to die out as one moves away from the perturbed end [15, 16]. It has another interesting property that the velocity of the trailing end is *always along the curve defining the flexible object*.

In the tractrix-based approach, the entire flexible object is discretized into a finite number of rigid segments. For a prescribed motion of the 'head' of the leading segment, the motion of the `tail' end of the same segment is computed, by employing the tractrix equation. This is fed as the input motion of the `head' of the subsequent segment and following the same procedure progressively, the `tail' motions are computed to the

trailing end. Since the entire flexible object is discretized into a finite number of rigid segments, the axial length of the flexible object is preserved. Due to the decaying motion property of the tractrix, the motion appears to be natural and intuitive [16]. The tractrix-based approach can *resolve the redundancy* and has the aforementioned two interesting properties. In reference [16], the tractrix-based approach is demonstrated for spatial motion. The main disadvantage of the tractrix-based approach is that the flexible object must be discretized into a finite number of *piece-wise rigid linear segments* and is not applicable for *smooth continuous curves*. In this paper we propose a formulation to simulate and visualize the motion of a flexible object so as to resolve the redundancy, using calculus of variations.

Length preserving nature aside, the most important characteristic of the tractrix solution is its property of inducing motion tangent to the curve at all points, thereby minimizing velocity of all the points at all instants of time. One can also argue that *velocity minimization implicitly implies that every point on the curve moves as little as possible*. The last assertion motivates us to solve the problem using optimization techniques. In addition to the minimization objective defined in [15], we present two other objective functions that yield similar results. We will be calling these parameters as *metrics*. It is shown that the tractrix-based solution is only one of the many possible length-preserving transformations for a given perturbation and it can also be obtained by minimizing certain appropriately chosen distance or motion metrics, which in turn depend on the given problem.

Above observations point towards a motion strategy wherein the perturbed curve tries to take a shape which minimizes its 'distance' metric from the original curve. However, the notion of 'distance measure or metric' between two configurations is rather abstract and depends on the nature of the problem to be solved. Based on the measure chosen, the motion derived will change and hence the metrics will be defined in a more problem-specific and precise mathematical form. In addition to proposing different measures, we also suggest two different optimization approaches, one based on sequentially optimizing the motion of individual rigid links with respect to the chosen norm and the other based on the single step optimization of a metric defined on the total curve instead of individual links. We call the first approach as *sequential optimization* and the second approach as *overall optimization*. The problem is posed in variational formulation which is also the motivation behind the overall optimization scheme mentioned earlier. The governing differential equations are also derived from the Euler-Lagrange equations of the system. Numerical simulations are carried out. As can be seen in the results, intuitive motion is obtained because of suitably handling the kinematics of motion.

In this paper, the entire analysis has been carried out for the planar motion of the rope. However, the approach can be generalized to spatial motions without any restrictions. The *fmincon* routine of MATLAB® is employed [17] for the numerical simulation studies throughout this paper.

A. Organization of the paper

The paper is organized in four sections. Section II describes the variational calculus-based formulation [18, 19] using the overall optimization approach and the sequential optimization approach. The simulation results are described and discussed in section III. Section IV contains the concluding remarks.

II. Formulations and Methods

A. Variational Formulation

It is usually believed that nature tries to optimize all processes by trying to minimize work done or energy loss. In a pure kinematic sense, we can reinterpret it as a minimization of movement in the direction of applied force or input motion. This motivated the concept of 'distance' metric approach.

While formulating the problem using variational calculus, we consider a curve of length l. The x and y coordinates of different points on the curve are given as functions of curve length s, namely $x(s)$ and $y(s)$. These unknown functions parametrically define the final configuration and also act as the optimization variables. The initial configuration of the curve is given by the known functions $x_0(s)$ and $y_0(s)$. Assume that the leading end moves from $(x_0(s), y_0(s))$ to $(x(l), y(l))$ as shown in Fig.1.
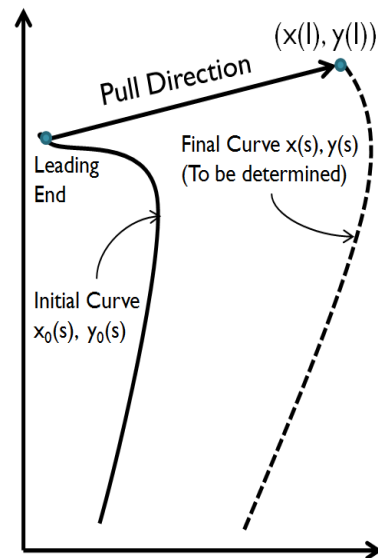

Fig. 1. Initial and displaced configurations

With the above given, the variational calculus problem is stated as follows:

$$\underset{x(s),\,y(s)}{Minimize}\int_0^l\sqrt{\left(x(s)-x_0(s)\right)^2+\left(y(s)-y_0(s)\right)^2}\,ds$$

Subject to

$$\Lambda:\int_0^l\sqrt{\left(\frac{dx}{ds}\right)^2+\left(\frac{dy}{ds}\right)^2}\,ds-l=0 \qquad (1)$$

Data:

$$x_0(s),\ y_0(s),\ x(s=l),\ y(s=l)$$

The functional here represents the area between the initial and final configurations. It is a candidate for measuring the distance between the curves and thus acts as the metric mentioned in the previous section. The minimization of the functional automatically implies that each point on the curve moves *as little as possible* when subjected to a perturbation at one end.

In (1), Λ is the Lagrange multiplier corresponding to the constraint that preserves the length of the curve as it is displaced. As the initial curve and the endpoint after perturbation are known, they are given as known input data in the variational statement.

Therefore the Lagrangian of the variational problem is given as:

$$L=\int_0^l\left\{\sqrt{(x(s)-x_0(s))^2+(y(s)-y_0(s))^2}\right\}ds+$$
$$\int_0^l\left\{\Lambda\sqrt{\left(\left(\frac{dx}{ds}\right)^2+\left(\frac{dy}{ds}\right)^2\right)}\right\}ds-\Lambda l$$
$$(2)$$

The corresponding Euler-Lagrange equations are

$$\frac{\partial L}{\partial x}-\frac{d}{ds}\left(\frac{\partial L}{\partial x'}\right)=0 \qquad (3)$$

$$\frac{\partial L}{\partial y}-\frac{d}{ds}\left(\frac{\partial L}{\partial y'}\right)=0 \qquad (4)$$

Where $x'=\dfrac{dx}{ds}$ and $y'=\dfrac{dy}{ds}$

By using (2.a) and (2.b) respectively we obtain the following expressions:

$$\frac{(x-x_0)}{\sqrt{(x-x_0)^2+(y-y_0)^2}}-\Lambda\frac{x''y'^2-x'y'y''}{(x'^2+y'^2)^{3/2}}=0 \qquad (5)$$

$$\frac{(y-y_0)}{\sqrt{(x-x_0)^2+(y-y_0)^2}}-\Lambda\frac{y''x'^2-x'y'x''}{(x'^2+y'^2)^{3/2}}=0 \qquad (6)$$

Eliminating Λ from (2.c) and (2.d), and subsequently simplifying the resulting expressions yield

$$\frac{y'}{x'}=\frac{dy}{dx}=\frac{x_0(s)-x(s)}{y(s)-y_0(s)} \qquad (7)$$

During the derivation of (7) it is assumed that $(x'^2+y'^2)^{3/2}$ cannot be equal to zero, which in turn implies the physical impossibility of any of the *infinitesimal length elements* shrinking to zero length.

B. *Overall Optimization*

Analytical solution for (7) is not possible for all but few simple curves. Hence, we solve the above variational problem using finite variable optimization wherein we discretize the curve into finite rigid link chain and give the perturbation in finite steps.

For overall optimization we employed the non-linear optimization routines available in MATLAB®. To reduce the number of constraints imposed on the problem, we changed our optimization variables from x(s) and y(s), as used in the variational formulation, to $\dfrac{dx}{ds}$. For any user defined initial curve, the program then extracts values of $\dfrac{dx}{ds}$ at finite number of points on the curve using forward difference. Since the individual infinitesimal length elements are assumed to be un-stretchable, $\dfrac{dy}{ds}$ is computed as

$$\frac{dy}{ds}=\sqrt{1-\left(\frac{dx}{ds}\right)^2} \qquad (8)$$

The discretized optimization problem can now be restated as:

$$\underset{\frac{dx}{ds}(i)}{Minimize}\sum_{i=1}^{n-1}\sqrt{\left(x(i)-x_0(i)\right)^2+\left(y(i)-y_0(i)\right)^2}\,\Delta s(i)$$

where, i=1 to n-1

Subject to

$$\Lambda:\sum_{i=1}^{n-1}\sqrt{\left(x(i+1)-x(i)\right)^2+\left(y(i+1)-y(i)\right)^2}-l=0$$

Data:

$$x_0(s),\ y_0(s),\ x(s=l),\ y(s=l)$$

where, n represents the number of discretized points considered along the length of the given curve and $\Delta s(i)$ represents the spacing between the ith and $(i+1)^{\text{th}}$ points.

Thus, following the previous argument, the functions $\dfrac{dx}{ds}$ will suffice to compute corresponding $\dfrac{dy}{ds}$ using (8) for every value of s during the motion. By knowing

the values of $\frac{dy}{ds}(s)$, $\frac{dx}{ds}(s)$, and $(x(s=0), y(s=0))$, we can fully define the configuration of the curve at a given instant of time.

C. Sequential Optimization

In this approach, the area minimization is applied at the elemental level and optimization propagates through the curve one segment at a time, i.e., sequentially.
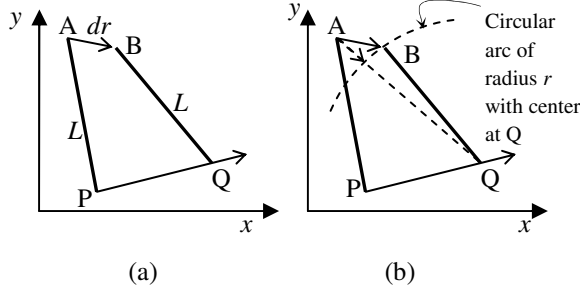

Fig. 2. (a) Elemental Area Minimization (b) Elemental Distance Minimization

Let the initial configuration of the rigid segment under consideration be AP. Assume the known input disturbance be PQ and the perturbed unknown configuration be BQ. The sequential optimization problem can then be stated in two ways.

1. Area Minimization Approach:

$$\underset{x_B, y_B}{Minimize}\ (\text{Area ABQP})$$

Subject to
$$|BQ| = L$$
Data:
     L, Step Length (PQ)

2. Distance Minimization Approach:

$$\underset{x_B, y_B}{Minimize}\ \sqrt{(x_A - x_B)^2 + (y_A - y_B)^2}$$

Subject to
$$\sqrt{(x_B - x_Q)^2 + (y_B - y_Q)^2} - L = 0$$

Data:
     L, Step Length (PQ)

Both the formulations for distance minimization and area minimization arrive at the same result as is clear from the Fig.2. For the distance moved by the trailing end to be minimized, the trailing end point B should be collinear with the radius vector $\vec{QA}$, which is also the condition for minimization of area of the quadrilateral ABQP. Application of the above procedure to a single rigid link with straight line motion applied at the leading end generates a tractrix as the resulting motion of the trailing end, as shown below in Fig.3.From this very fact, it can be concluded that sequential element level optimization leads to conventional tractrix-based solutions as mentioned in the introductory part of this paper.
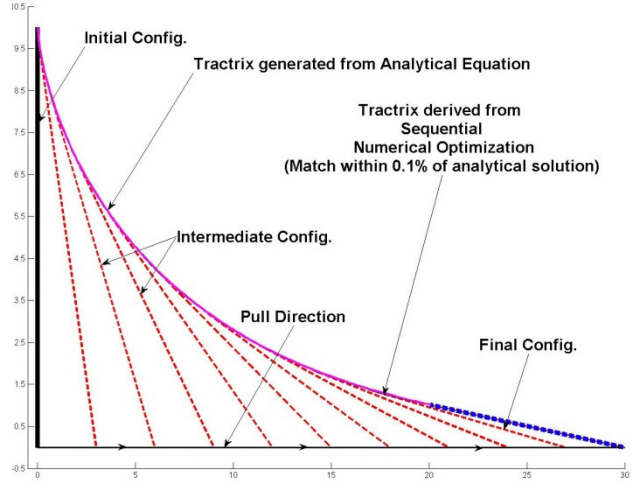
Fig. 3. Comparison of curves obtained using analytical equation of a tractrix and the sequential numerical optimization

To summarize, sequential optimization implies that, given an input curve, the configuration of the link that is nearest to perturbed end is obtained using area or distance minimization, the new position of the link's endpoint is extracted and given as input perturbation to the following link and then this process is *sequentially applied* until the last link is reached. Thus, we get the new curve. In Fig.4 a known perturbation is given to the nth (last) point of the initial curve. Sequential optimization determines the motion of the $(n-1)^{th}$ link using the methods described above. This gives the locus of the $(n-1)^{th}$ point which is used as the known perturbation while determining the motion of the $(n-2)^{th}$ link. Use of this method up to the 2nd point will give us the motion of the entire curve.

III. Results and Discussions

As mentioned earlier, to quantify the abstract notion of *distance* between two configurations, we have selected different metrics defined between the configurations. We now present five chosen distance measures labeled as metric 1 to 5.
Where,

a) Metric 1: Sum of the squares of the distances (m^2)

b) Metric 2: Area traced (m^2)

c) Metric 3: Sum of squares of joint rotations (rad^2)

d) Metric 4: Weighted square sum of distances (m^3)

e)   Metric 5: Weighted square sum of joint rotations (m.rad^2)

Metric 1 represents sum of the squares of the distances between the corresponding points lying on the two configurations. Metric 2 represents the area between the two configurations. Metric 3 represents the sum of squares of joint rotations while transforming from initial to perturbed configuration. Metric 4 represents the weighted square sum of distances moved by discretized points from initial to final configuration. Metric 5 represents the weighted square sum of joint rotations from initial to final configurations. The weights used here are the curve lengths measured from perturbed tip to the respective discretized points.
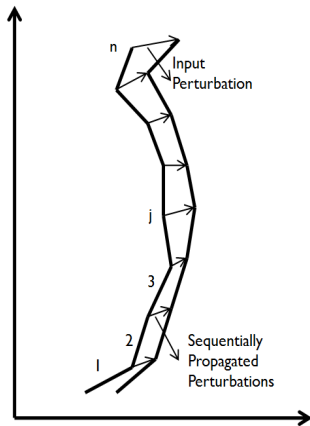
Fig. 4. Pictorial illustration of sequential optimization technique

While the first three metrics are chosen to provide adequate measures of distance between two curves in general sense, the last two have been chosen specifically with an objective of minimizing the closeness measures for points away from the perturbed tip so that motion is constrained to the neighborhood of the perturbed tip.

Values of these metrics, calculated for a parabola, using sequential and overall optimization routines for single step as well as multi step perturbation are shown in TABLE 1. In the case of multi-step methods we used five steps with perturbation $(0.1, 0.1)$ unit/step and for single step a perturbation of $(0.5, 0.5)$ unit is given to the end point.

Metric	Overall Optimization		Sequential Optimization	
	Single step	Multi step	Single step	Multi step
Metric 1	8.6601	8.6931	8.9479	9.3228
Metric 2	2.9847	2.9982	3.0491	3.1126
Metric 3	0.1099	0.1526	0.0968	0.1430
Metric 4	19.1153	19.2260	20.0979	21.1787
Metric 5	0.4606	0.6406	0.3146	0.4532

TABLE 1. Comparison of different metrics

Fig. 5. shows the optimized perturbed configurations derived for a parabola using different optimization strategies described so far. Metric 2 was used as objective functions in all of the cases.
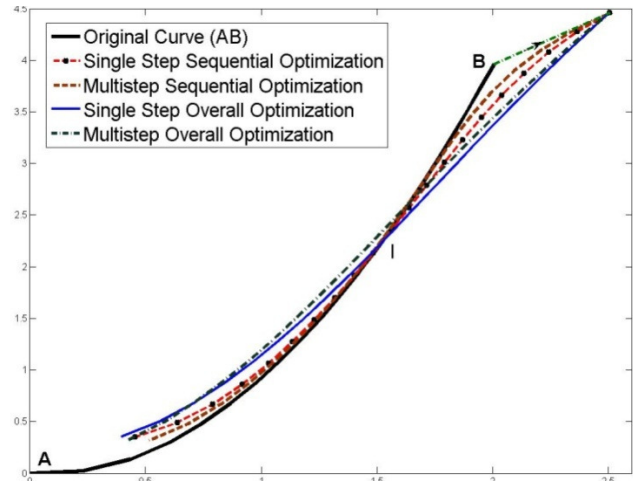

Fig. 5. Different optimization techniques applied on a parabola

As can be observed from TABLE 1, while metrics 1 and 2 are low for overall optimization with single-step perturbation, metric 3 gets minimized for sequential optimization with single-step perturbation. Proceeding along the same lines, while metric 4 seems to favor sequential optimization with multistep perturbation, metric 5 shows that the weighted squares of joint rotations away from the perturbed tip are monotonically decreasing for the curves derived using sequential optimization and the same has been plotted in Fig.6. from which it can be inferred that sequential optimization (i.e. tractrix-based) solutions induce the least amount of joint rotation on points away from the perturbed tip, as most of the motion is taken up by joints closer to the leading end of the rope. For the same reason, metric 5 gets minimized for sequential elemental optimization solution. This reveals a common characteristic of all the optimization solutions presented here that the curve length-weighed joint rotations from the initial to the perturbed configuration decrease monotonically and they asymptotically approach zero as one moves away from the perturbed point. Another important outcome of the simulation is that, although the tractrix-based solution matches exactly with the elemental sequential optimization solution for any given flexible straight line input curves or input curves concave with respect to the given perturbation input (which is the case as shown in Fig. 8., a sine curve). The same is not true if given input curve is convex with respect to given perturbation direction (which the case in Fig. 5., a parabola). In such a scenario, as one can see from the results, that the optimization solution will intersect with the initial input curve AB at a point I. While the portion BI will follow motion matching with the tractrix-based solution, the portion AI exhibits a completely different behavior which deviates from a tractrix-based solution. The exact reasons

for this, needs to be investigated in detail at a later point of time.

The results indicate that depending on the nature of the objective function, the resulting perturbed configuration depends on the choice of optimization strategy, whose choice, in turn rests on the minimization objective of the problem in hand. An alternate approach to the problem would have been to make all of these metrics (specifically 3,4 and 5) as objective functions for the optimization problem, but owing to the highly non-linear nature of the objective function and the subsequent convergence issues of the numerical routine used, we opted for numerical evaluation of metrics as shown above.

finite input perturbation. As can be observed from the figures, sequential and overall optimization gives entirely different final configuration for the same input curve and perturbations. Similarly, the single-step and multistep optimization routines also yield substantially different solutions.

In addition, to shows the applicability of the methods described so far to any generic scenario, simulation results have been given for motion derived in response to an arbitrary input perturbation at the 'leading end' of the curve are shown in Fig. 16 and Fig. 17.
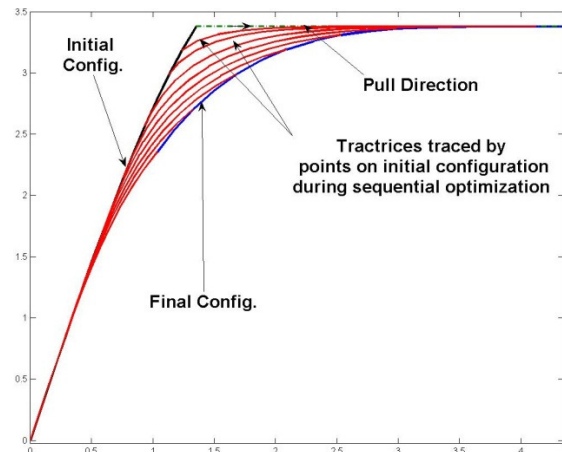

Fig. 6. Monotonically decreasing nature of weighted squares of joint rotations for the optimized final configurations

Fig. 7. Tractrices obtained in case of a straight rope

The results found indicate that depending upon the nature and objective of the problem in hand, proper norm needs to be chosen. For example, if the application is for a flexible robotic manipulator chain, the main objective will be to minimize the joint rotations so as to minimize motor actuation and power consumption, in which case metric 3 may be employed. However, if the problem is connected with trajectory planning of a locomotive, then the importance shifts to minimizing the area traced by the locomotive over time. On the other hand, an objective of distance minimization will yield the classical tractrix-based solution, as can be noted from the Fig. 7 where the above mentioned curves generated during the motion from initial configuration to perturbed configuration are shown in dotted lines. This proves our claim that the tractrix is one of the many possible solutions for a given perturbation and imposed length preserving nature of motion.

Next we are giving more cases considering straight line and sine curve as the initial configurations in Fig. 7-Fig. 14. The continuous curves shown are the initial input curves; the pull direction is the predefined direction of perturbation to the leading end of the curve, indicated by the chain line. The dotted curves show the intermediate and final configurations assumed by the curve after each
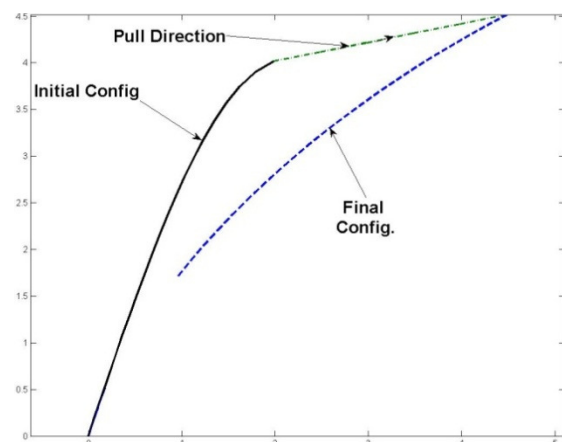

Fig. 8. Initial and Final configuration of a Sine curve subjected
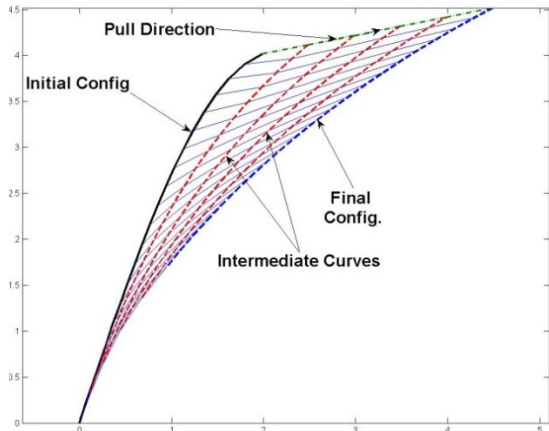To multi-step overall optimization

Fig. 9. Overall optimization for a sine curve subjected to multistep perturbation (with intermediate configurations)
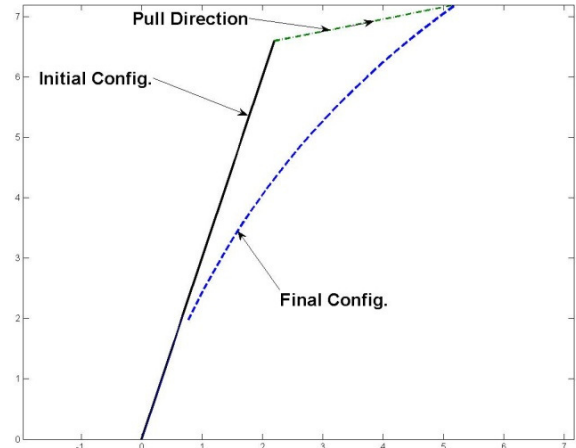

Fig. 12. Initial and Final configuration of a Straight Line subjected To multi-step overall optimization
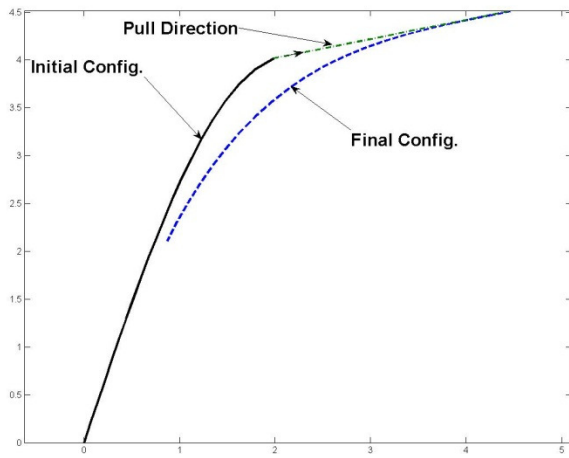

Fig. 10. Initial and Final configuration of a Sine curve subjected To multi-step sequential optimization
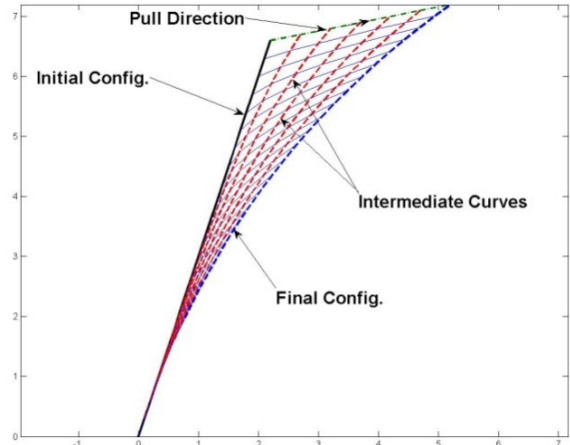

Fig. 13. Overall optimization for a straight line subjected to multistep perturbation (with intermediate configurations)
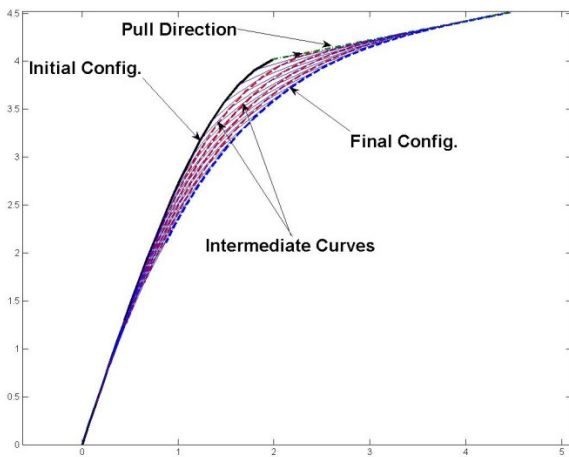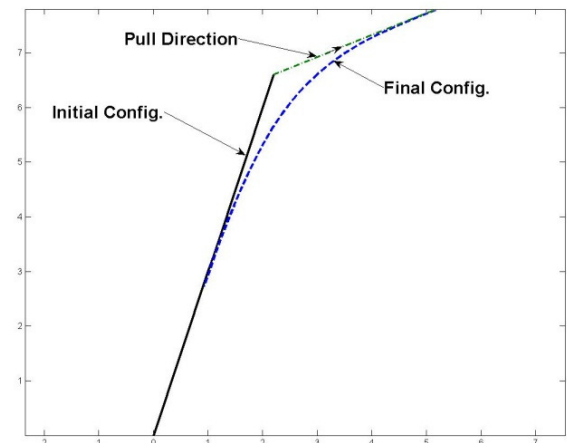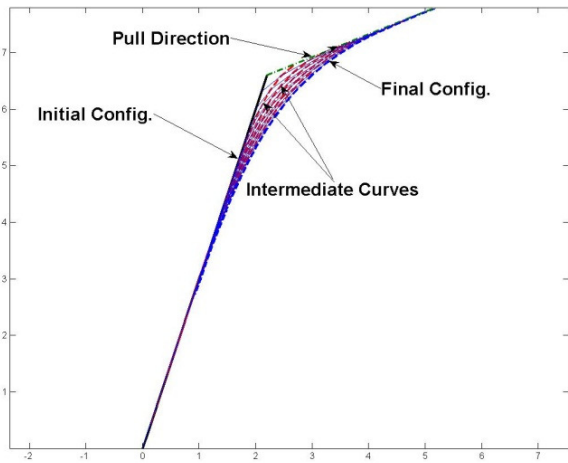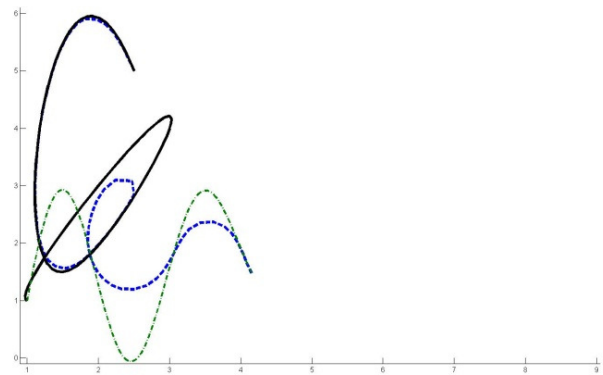

Fig. 11. Sequential elemental optimization for a sine curve subjected to multistep perturbation (with intermediate configurations)
.

Fig. 14. Initial and Final configuration of a Straight Line subjected To multi-step sequential optimization

Fig. 15. Sequential elemental optimization for a straight line subjected to multistep perturbation (with intermediate configurations)
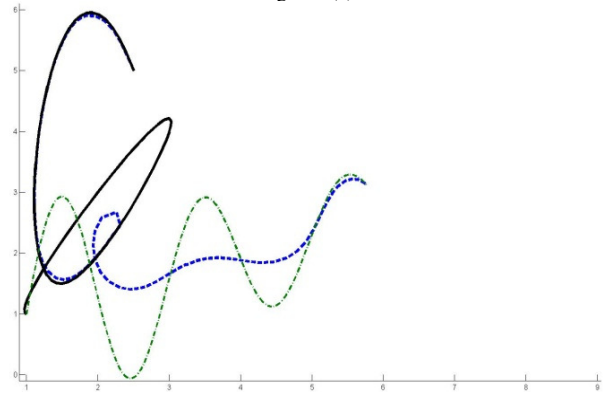

Fig. 16. (c)
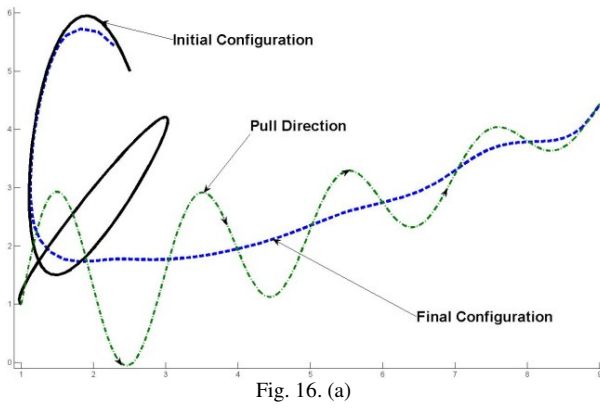
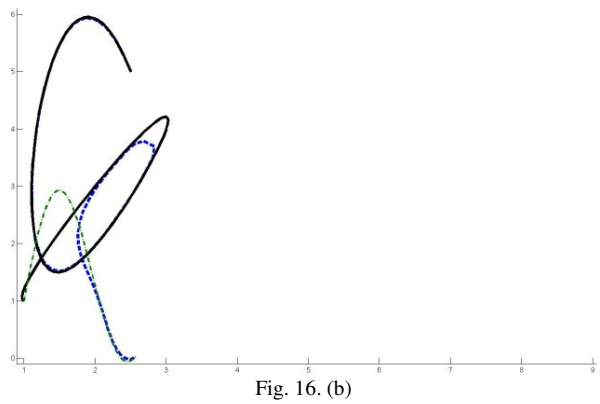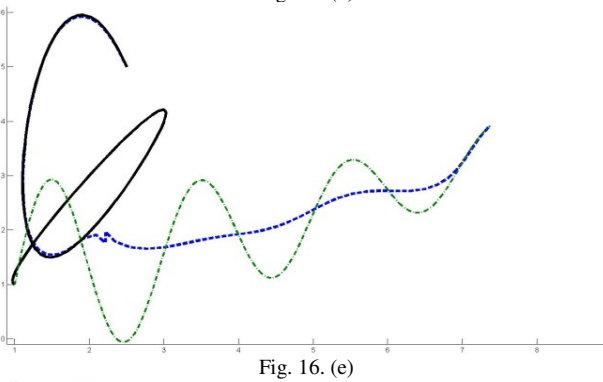Fig. 16. (d)

Fig. 16. (e)

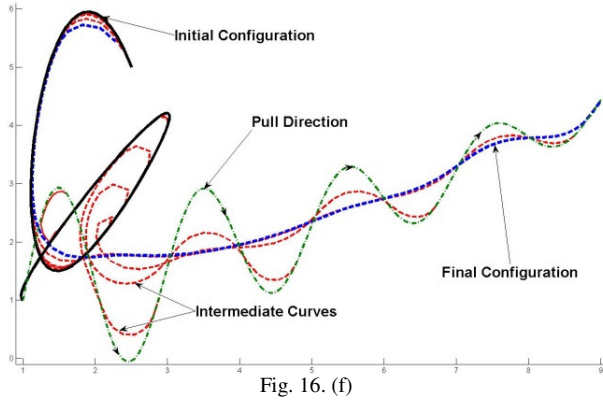Fig. 16. (a)

Fig. 16. (b)

Fig. 16. (f)

Fig.16. Sequential elemental optimization for an arbitrary curve subjected to multistep generic perturbation (e.g. sinusoidal). (a) shows the initial and final configurations along with the generic pull direction. (b)-(e) show intermediate configurations during motion showed in (a).
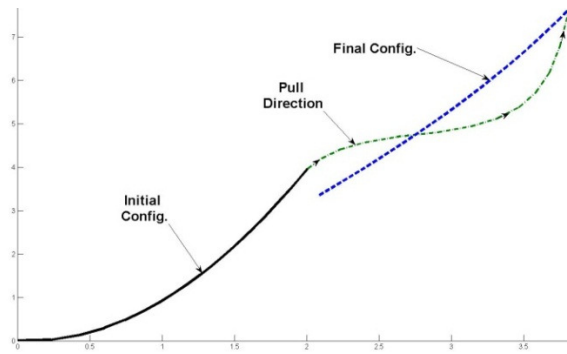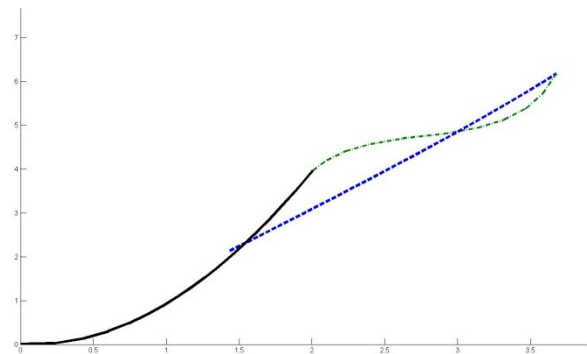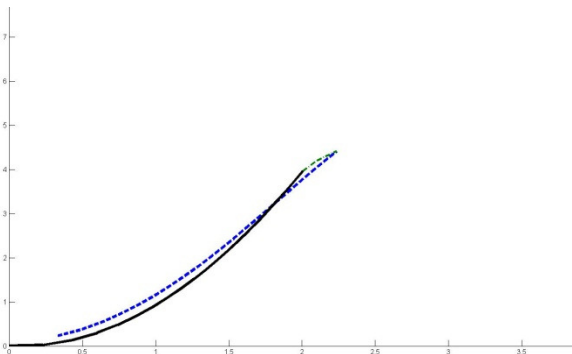
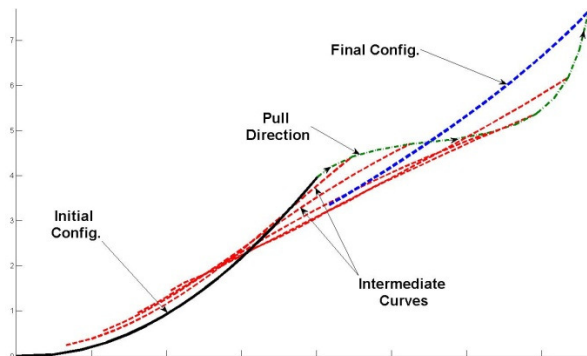Fig. 17. (a)

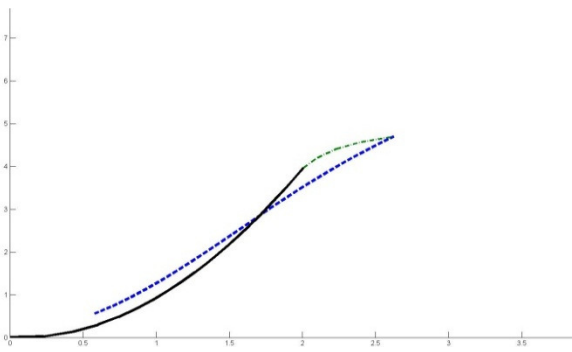Fig. 17. (b)

Fig. 17. (c)

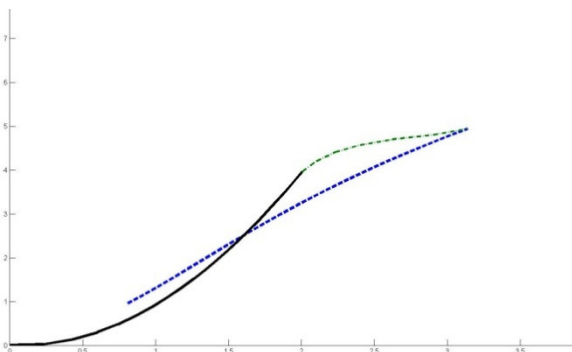Fig. 17. (d)

Fig. 17. (e)

Fig.17. (f)

Fig.17. Overall optimization for an arbitrary curve subjected to multistep generic perturbation. Fig. 17. (a) shows the initial and final configurations along with the generic pull direction. Fig. 17. (b), (c), (d), and (e) show intermediate configurations during motion showed in (a). Fig. 17. (e) shows the initial and final configurations with the loci of the intermediate joints

IV. Conclusion and Future Work

A new approach, based on calculus of variation, for the simulation and visualization of the motion of a flexible object is proposed in this paper. The proposed approach can also be used for redundancy resolution in hyper-redundant robotic manipulators. The approach is a generalization of an algorithm developed for piece-wise linear segments using a classical curve called the tractrix. It is shown that the tractrix-based approach is one of the many possible length-preserving transformations for a smooth curve. An important feature of the proposed algorithms is that it is a *kinematics-based* solution and it does not require assuming values for mass, stiffness, or damping of the flexible object which are required for simulations based on dynamics. Since approach is solely kinematics and geometry based, it can be applied to simulation and visualization of motion of generic flexible objects such as snakes, chains, etc. The minimization property leads to a more natural motion of these objects.

The paper presents various objective functions for the minimization. Based on the objective function employed, the solution to the problem changes and this approach

can give the optimized and appropriate solutions for any given objective, which in turn will be decided by the problem in hand.

V. References:

[1] J. Baillieul, J. Hollerbach, C.W. Brockett, Programming and control of kinematically redundant manipulators, in: Proceedings of the 23rd IEEE Conference on Decision and Control, 1984, pages 768–774.

[2] A. Liegeois, Automatic supervisory control of the configuration and behavior of multi-body mechanisms, IEEE Transactions, Systems, man and Cybernetics 7 (1977), pages 868–871.

[3] O. Khatib, Real-time obstacle avoidance for manipulators and mobile robots, in: Proceedings of the IEEE International Conference on Robotics and Automation, 1985, pages 500–505.

[4] J.M. Hollerbach, K.C. Suh, Redundancy resolution of manipulators through torque optimization, IEEE Transactions, Journal of Robotics and Automation3 (1987), pages 308–316.

[5] T. Yoshikawa, Manipulability of robotic mechanisms, The International Journal of Robotics Research 4 (1985), pages 3–9.

[6] C.A. Klein, C.H. Huang, Review of the pseudo-inverse for control of kinematically redundant manipulators, IEEE Transactions on Systems, Man, and Cybernetics SMC-13 (3) (1983), pages 245–250.

[7] Y. Nakamura, Advanced Robotics: Redundancy and Optimization, Addison-Wesley, 1991.

[8] K. Ward, F. Bertails, T. Kim, S. R. Marschner, M. P. Cani, M. C. Lin, A Survey of Hair Modeling: Styling, Simulation, and Rendering, IEEE Transactions on Visualization and Computer Graphics (TVCG) (13) (2007), pages 213-234.

[9] U. Kuhnapfel, H. K. Cakmak, H Maass, Endoscopic surgery training using virtual reality and tissue simulation, Computers and Graphics, 24(2000), pages 671-682.

[10] H. Kang and J. T. Weng, Robotic knot tying in minimally invasive surgery, Proceedings of IEEE/RSJ Int. Conference on Intelligent Robots and Systems, 2002, pages 1421-1426.

[11] D. K. Pai, STRANDS: Interactive Simulation of Thin Solids using Cosserat models, Computer Graphics Forum (21)(2002) 347-352

[12] R. Barzel, Faking Dynamics of Ropes and Springs, IEEE Computer Graphics and Applications (17) (1997), pages 31-39.

[13] http://mathworld.wolfram.com/Tractrix.html

[14] Steinhaus, H., Mathematical Snapshots, 3rded. New York: Dover (1999) ISBN:0-486-40914-7.

[15] D. Reznik, V. Lumelsky, Sensor-based motion planning in three dimensions for a highly redundant snake robot, Advanced Robotics **9** (3) (1995), pages 255–280.

[16] S. Sreenivasan, P. Goel, A. Ghosal, A real-time algorithm for simulation of flexible objects and hyper-redundant manipulators, Mechanism and Machine Theory 45 (2010), pages 454–466.

[17] http://www.mathworks.com/help/

[18] I. M. Gelfand, S. V. Fomin, Calculus of Variations, ISBN: 0-486-41448-5.

[19] D. R. Smith, Variational Methods in Optimization, ISBN: 0-486-40455-2.